UDK519.63+533.6

Numerical model of an axisymmetric current of the heat carrier in collectors for fuel elements of an axial blowing

S. V. Zhuchenko
V. N. Karazin Kharkov National University, Ukraine

A two-dimensional hydrodynamic problem concerning the gaseous coolant flow in the axisymmetric distributing and gathering collectors for a bulk heat-generating element for a fast-neutron nuclear reactor is solved numerically. Gas flow pressure in such collectors is determined and by its distribution, the longitudinal resistance coefficient magnitude in various cross-sections of such collectors is calculated. Numerical experiments, in order to examine the influence of coolant flow vorticity degrees in collectors on the magnitude of the resistance coefficients, are performed. The band diagrams for isobars and individual motion trajectories of free vortices inside collectors are given as well.

***Key words**: distributing and gathering collectors; gas flow velocity; gas flow pressure; resistance coefficient; total and free vortices.*

*Ч*исельно вирішується 2-х мірне завдання гідродинаміки про течію газового теплоносія в осесиметричних розподільному і збірному колекторах для насипного тепловиділяючого елементу в ядерному реакторі на швидких нейтронах. Визначається тиск газового потоку в таких колекторах і по його розподілу обчислюється величина подовжнього коефіцієнта опору в різних поперечних перерізах таких колекторів. Проводяться чисельні експерименти по вивченню впливу мір завихореності газового потоку в колекторах на величину таких коефіцієнтів опору, наводяться графіки смуг для ізобар і траєкторії переміщення окремих вільних вихорів усередині.

Ключові слова:розподільний і збірний колектора; швидкість газового потоку і тиск; коефіцієнт опору; сумарні і вільнівихори.

Численно решается 2-х мерная задача гидродинамики о течении газового теплоносителя в осесимметричных распределительном и сборном коллекторах для насыпного тепловыделяющего элемента в ядерном реакторе на быстрых нейтронах. Определяется давление газового потока в таких коллекторах и по его распределению вычисляется величина продольного коэффициента сопротивления в различных поперечных сечениях таких коллекторов. Проводятся численные эксперименты по изучению влияния степеней завихрённости газового потока в коллекторах на величину таких коэффициентов сопротивления, приводятся графики полос для изобар и траектории перемещения отдельных свободных вихрей внутри коллекторов.

Ключевые слова: распределительный и сборный коллектора; скорость газового потока и давление; коэффициент сопротивления; суммарные и свободные вихри.

Introduction

At the 6-th conference AMiTaNS'14 in Bulgaria I presented my report entitled "Numerical simulation of gas dynamics and heat exchange tasks in fuel assemblies of the nuclear reactors". In this report I examined a numerical model of a coolant average flow in fuel assembly consisting of bulk heat-generating elements for small nuclear reactors. Nuclear fuel is placed inside spherical heat-generating microelements (further MHG elements) under protective cover. These MHG elements are filled into a cylindrical annular domain. Helium is used as a coolant. Using a system of

distributing collectors, gas is blown through the permeable bottom plates of such areas and, being heated in the HG elements, assembles in the inner tube due to a system of gathering collectors as it is showed in Fig.1. Average flow inside the HG elements and collectors is assumed to be axisymmetric. That's why, inside the HG elements it is two-dimensional, but in collectors, because of a small size of the cross-sections and in order to simplify and speed up the computation process, the flow is assumed to be one-dimensional. Flow parameters in collectors have been calculated using the functions - distribution of the longitudinal components of the coolant momentum vector of movement quantity, density, pressure and temperature of the gas in gathering collectors. In the HG element, after each iterative process step in time, connection between these values in collectors has been determined by a system of fixed one-dimensional finite-difference equations of mass, energy and movement quantity balance conservation, compiled for elementary volumes dΩ.

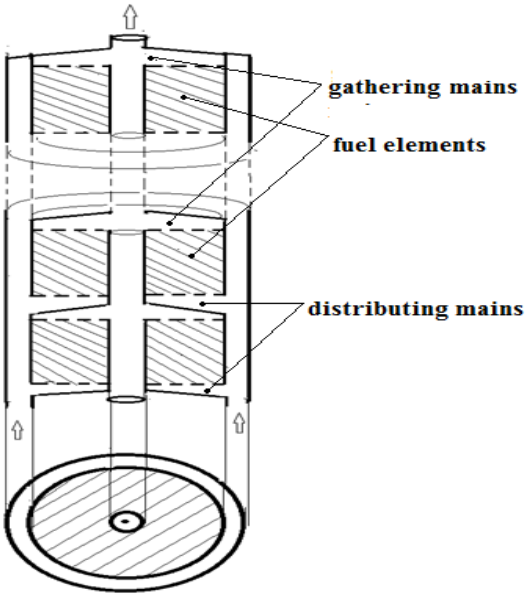

Fig. 1. Fuel assembly of the HG elements.

So, for a gathering collector, finite-difference equation of conservation of momentum and movement quantity is:

$$\left(\rho v^2 S\right)_j^g - \left(\rho v^2 S\right)_{j+1}^g + \left(P_j^g - P_{j+1}^g\right) S_{j+\frac{1}{2}}^g - f_g \left(\rho |v| v\right)_{j+\frac{1}{2}}^g \Im_j^g +$$

$$+ \left(\rho v_r u_z\right)_{M+\frac{1}{2}, j} S_{2j-1}^{tg} + \left(\rho v_r u_z\right)_{M+\frac{1}{2}, j+1} S_{2j}^{tg} = 0. \qquad (1)$$

where P_j^g – pressure on the gathering collector cross-section j;

ρv_j – momentum vector of movement quantity longitudinal component;

v_j – velocity vector longitudinal component;

S^{tg}_{2j} – boundary area between HG element cell $(M+\frac{1}{2}, j+1)$ and volume cell $\Im^g_j$ in the gathering collector;

$(\rho v_r u_z)_{M+\frac{1}{2},j}$ – intensity of the component of the movement quantity vector, transmitted by a gas flow from the HG element to the gathering collector, which coincides with a flow direction in the collector;

f_g – resistance coefficient in the gathering collector;

The resistance coefficient in gathering and distributing collectors, used for the formula (1), is determined by physical or numerical experiments which are conducted using the solutions of two-dimensional hydrodynamic problems for collectors. This report is dedicated to the solution of these problems.

1. Two-dimensional numerical model of the gathering collector hydrodynamics.

In the HG element, the collector flow of the coolant in axial pumping cartridges is perpendicular to the one-dimensional flow in the collectors. That's why in reality, the coolant flow is essentially two-dimensional and highly swirling, which significantly affects the drag coefficient magnitude in the collectors. Resistance apparently is greatly varied in various sections of the collector. According to this, I propose an effective method for calculating of the coolant two-dimensional flow throughout the gathering collector. As a result of these calculations the pressure distribution within the gathering collector is expected to be obtained and as a result we can clarify how the values of the drag coefficient in the one-dimensional simulation model of the collectors, used in the cartridge calculations, change.

Formulation of the problem.

The axisymmetric flow of an incompressible inviscid gas in the region, the axial section of which is shown on Fig. 2, is considered. Impermeable walls OA, BCDE and grid AB, connecting HG element and collector are replaced by continuous layers of circle vortices. The field of velocities, induced by these vortex layers, satisfies the Eulere equations for an ideal fluid in the entire region of coolant flow. Tension of the vortex layers $\gamma(z,r)$ is determined from the condition of the impenetrability of the walls, for a given velocity profile V_z on the grid AB, as well as from the rate of input-output flow balance at the inlet AB and at the outlet EF. Vortex layer from the grid is entrained by the flow into the region and as a result becomes a vortex as well. Separation of the boundary layer on the sharp edge D is being modeled by vortex sheet which is trailing continuously along CD line thence. Thereby the requirements of the Chaplygin-Zhukovsky hypothesis about finite values of velocity and pressure in the entire flow region are satisfied. Practical implementation of the proposed scheme is based on the method of the discrete vortices. The transition from the continuous distributions of flow parameters and the processes of their change in time to discrete one [2] is realized in the numerical calculations.

Vortex layer is modeled by a system of discrete vortex rings. Continuous process of changing the boundary conditions in time is replaced by a stepped one. It is supposed that the boundary condition changes abruptly in some calculated moments $t = 0, t_1, \ldots, t_n$, but in the intervals between these moments remains unchanged and equal to the value at the beginning of each interval.

Vortices located on the impermeable boundary model both attached and free vortex layer and therefore they are called a total vortex layer. Discrete vortices that model free vortex layer on the grid AB and vortex sheets trailing edge D, are called free. Vortices on the boundary lines are placed along the circle lines and located on the approximately equal distance from each other along the generating line and the control points are in the middle of the lines between them. Herewith there are vortices at all border kinks. Free vortex that is closest to the edge D and the corresponding control point are placed on the cone, tangent to the boundary at this location.

Algorithm of the method of discrete vortices.

Fig.3 shows an example of the placement of discrete vortices and control points. Let's enter cylindrical coordinates $0zr\theta$. (See Fig.3) and proceed to the dimensionless circulation, speed, and coordinates:

$$g = \frac{G}{U_0 L_0}, \quad \vec{w} = \frac{2\pi\vec{V}}{U_0}, \quad \vec{v} = \frac{2\pi\vec{V}L_0}{G}, \quad z = Z/L_0, \quad r = R/L_0. \quad (2)$$

This shows that two types of dimensionless velocity $\vec{w}$ and $\vec{v}$ are used. The relation between them: $\vec{w} = g\vec{v}$.

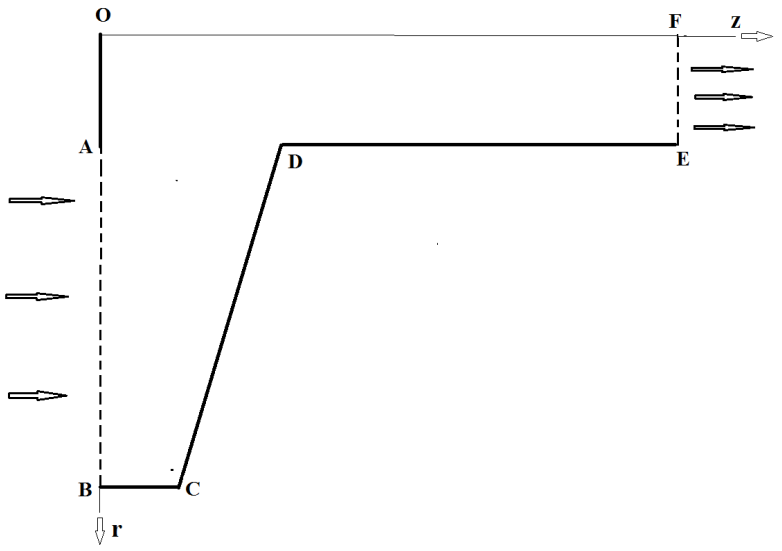

Fig. 2 Axial section area

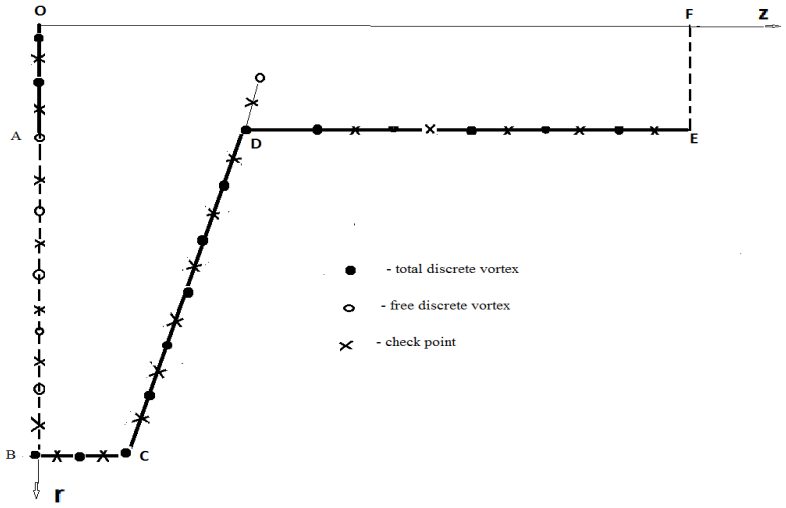

Fig. 3. Placement of vortexes and check points at the start of the computation

Consider a circular vortex of radius r_1 located in plane $z = z_1$. Axial and radial components of the dimensionless velocity is induced by this vortex at coordinates z_0, r_0 define by the formulas [2]:

$$v_z = -\frac{r_1}{2}\int_0^{2\pi} \frac{(r_1 - r_0\cos\theta)d\theta}{\left[(z_0 - z_1)^2 + r_1^2 + r_0^2 - 2r_1 r_0\cos\theta\right]^{3/2}} \tag{3}$$

$$v_r = -\frac{(z_0 - z_1)\ r_1}{2}\int_0^{2\pi} \frac{\cos\theta\, d\theta}{\left[(z_0 - z_1)^2 + r_1^2 + r_0^2 - 2r_1 r_0\cos\theta\right]^{3/2}} \tag{4}$$

Dimensionless speeds v_z and v_r can be expressed in terms of complete elliptic integrals of the first and second kind, K and E with module

$$k^2 = \frac{4r_1 r_0}{(z_0 - z_1)^2 + (r_0 - r_1)^2} \tag{5}$$

In this

$$K = \int_0^{\pi/2} \frac{d\psi}{\sqrt{1 - k^2\sin\psi}}, \quad E = \int_0^{\pi/2} \sqrt{1 - k^2\sin\psi}\, d\psi \tag{6}$$

As a result the expressions (3) and (4) are reduced to the following form:

$$v_z(z_0, r_0, z_1, r_1) = \frac{1}{\sqrt{(z_0 - z_1)^2 + (r_0 - r_1)^2}} \left(\frac{2 - k^2}{1 - k^2} E - 2K - \frac{r_1 k^2}{r_0 + k^2} E \right) \quad (7)$$

$$v_r(z_0, r_0, z_1, r_1) = -\frac{(z_0 - z_1)}{r_0 \sqrt{(z_0 - z_1)^2 + (r_0 - r_1)^2}} \left(\frac{2 - k^2}{1 - k^2} E - 2K \right) \quad (8)$$

The system of M vortices with intensity g_i, radius r_i which are located in the region of the flow in the plane $z = z_i$ $(i = 1,2,...,M)$ at an arbitrary point z_0, r_0 induce the vector of velocity $\vec{w}(z_0, r_0) = (w_z, w_r)$ which is defined by the formula:

$$\vec{w}(z_0, r_0) = \sum_{i=1}^{M} g_i(z_i, r_i) \vec{v}(z_0, r_0, z_i, r_i) \quad (9)$$

Using the equation (9) we can write down the expression for the normal component of the velocity vector at all control points of the boundary (z_k, r_k) and equate them to the known values of these quantities $w_n = f_n(z_k, r_k)$. On the impermeable boundary: $f_n(z_k, r_k) = 0$, and on the grid AB they are given: $f_n = f(r_k)$. In the result we obtain M-1 equation to determine the unknown values of circulation g_i :

$$\sum_{i=1}^{M} g_i \left[v_z(z_k, r_k, z_i, r_i) n_z(z_k, r_k) + v_r(z_k, r_k, z_i, r_i) n_r(z_k, r_k) \right] = f_n(z_k, r_k), \quad (10)$$

$k = 1,2,...,M-1.$

The missing equation can be obtained with writing the balance equation for volumetric flow for cross sections AB and EF, i.e. $R_{EF} = R_{AB}$. The flow through the cross section AB is determined by a given distribution of the normal component of the velocity at the control points of the border, and by EF – the distribution of the normal velocity component, which is defined by the formula (9). As a result, we have:

$$\sum_{i=1}^{M} g_i \sum_{j=1}^{L} v_z(z_j, r_j, z_i, r_i) S_j^{EF} = \sum_{k=P_1}^{P_2} f(r_k) S_k^{AB} \quad (11)$$

The system of linear equations (10–11) determines the intensity of the vortices g_i and thereafter by the formula (9) it is possible to calculate the flow rate at any point in the flow region, and hence the velocity of free vortices which are entrained by it. The

new coordinates of the free vortices located at the point (z_s, r_s) are defined, integrating the system of ordinary differential equations in the time interval (τ_0, τ_1):

$$\frac{dz_s}{d\tau} = w_z(z_s, r_s), \quad \frac{dr_s}{d\tau} = w_r(z_s, r_s). \tag{12}$$

The period (τ_0, τ_1) is chosen in view of the fact that the offset of the fastest vortex does not exceed the distances between the total vortices on the impermeable border.

By the assumption of the absence of vortices dispersion, the intensity of descended free vortices remains unchanged during the whole time of resolution.

On the next steps of the resolution, the summands of the free vortices coming down the stream are additionally present in the equations (10) and (11). The circulation of these vortices is known, thus, these terms are transferred to the right side of the equations, and as a result they are converted to the form:

$$\sum_{i=1}^{M} g_i \left[v_z(z_k, r_k, z_i, r_i) n_z(z_k, r_k) + v_r(z_k, r_k, z_i, r_i) n_r(z_k, r_k) \right] = f_n(z_k, r_k) -$$

$$- \sum_{n=1}^{N} \gamma_n \left[v_z(z_k, r_k, z_n, r_n) n_z(z_k, r_k) + v_r(z_k, r_k, z_n, r_n) n_r(z_k, r_k) \right] \tag{13}$$

$$(k = 1,2,\ldots, M-1)$$

$$\sum_{i=1}^{M} g_i \sum_{j=1}^{L} v_z(z_j, r_j, z_i, r_i) S_j^{EF} = \sum_{k=P_1}^{P_2} f(r_k) S_k^{AB} - \sum_{n=1}^{N} \gamma_n \sum_{j=1}^{L} v_z(z_j, r_j, z_n, r_n) S_j^{EF}. \tag{14}$$

Having resolved the system (13–14) for g_i by formula (9) we determine the velocity vectors of all free vortices, and integrating system (12) we find that their displacement with the flow.

By repeating this process, we carry out numerical simulation of unsteady flow of coolant in a typical section of the gathering collector of the cassette of HG elements.

Determination of the pressure in the gathering collectors.

By the known distribution of flow velocities it is possible to obtain the pressure distribution in the gathering collector and thereby determine the value of its flow resistance both as a whole and at its separate areas. For this we can use the Euler equations for axisymmetric flow in cylindrical coordinates [3]:

$$\begin{aligned} \frac{\partial w_r}{\partial t} + w_r \frac{\partial w_r}{\partial r} + w_z \frac{\partial w_r}{\partial z} &= -\frac{\partial P}{\partial r} \\ \frac{\partial w_z}{\partial t} + w_r \frac{\partial w_z}{\partial r} + w_z \frac{\partial w_z}{\partial z} &= -\frac{\partial P}{\partial z} \end{aligned} \tag{15}$$

From the equations (15) and the continuity equation is easy to obtain the Poisson equation for the pressure in cylindrical coordinates:

$$\frac{\partial^2 P}{\partial r^2}+\frac{1}{r}\frac{\partial P}{\partial r}+\frac{\partial^2 P}{\partial z^2}=-\left[\left(\frac{\partial w_r}{\partial r}\right)^2+2\frac{\partial w_r}{\partial z}\frac{\partial w_z}{\partial r}+\left(\frac{w_r}{r}\right)^2+\left(\frac{\partial w_z}{\partial z}\right)^2\right] \quad (16)$$

The equations (31) define $grad\ P$ on the boundary and together with (16) are the Neumann problem for the pressure in the reservoir.

To solve this system, to the left side of equation (16) we formally add the transient member $\frac{\partial P}{\partial \tau}$ and in the resulting equation and the equations (14) we go to the finite differences. The resulting system of non-stationary equations we resolve via the "classical" method.

Solving the particular problem for the pressure in the gathering collector is a bit simpler than the standard Neumann boundary value problem. On the collector exit, the pressure value is known according to the problem conditions (section of the border EF in Fig. 3). This gives a powerful stabilizing effect and the decision does not "float", as it usually happens in the Neumann problem.

2. Results of the numerical experiments.

In the numerical experiments I simulated and examined vortex formation processes in collectors and the connection of a field vorticity degree with pressure distribution. Using these pressure distributions, the coolant flow resistance coefficients in the various sections of the collector have been calculated. For this purpose, obtained two-dimensional pressure distribution in the collector has been averaged over the cross-section according to the primary flow. Using one-dimensional pressure distribution in the gathering collector, obtained according to the formula (1) in the introduction of this article, we can calculate the drag coefficient functions tables at all points of the discrete network placed on the border of the collector and HG element. Similar formulas have been used in the border places of the distributing collector and HG element. The drag coefficients on the distributing collector inlet and the gathering collector outlet have been also determined. A pipe section with the radius Ro is the outlet for the gathering collector (area between D and E points in the Fig. 2). In the distributing collector, the inlet is an annular cylindrical slit with the radius R_2 and the length L. Resistance coefficient is calculated by the formula:

$$P_{in}-P_{ex}=f_g\rho v^2 L \quad (17)$$

P_{in}, P_{ex} – flow average pressure on the inlet and outlet of a zone, where resistance f_g is determined;

ρ – density and v –velocity of the coolant in the collector, which is longitudinal to the primary flow.

Free vortices in the inner area of the collector seriously affect the pressure distribution in it. We can see it clearly in Fig. 4, where equal pressure interval bands in the gathering collector are shown: Fig. 4a - the case when there are no such vortices yet and Fig. 4b - the case, when we already have 138 vortices.

Let me explain these pictures. Axial section of the gathering collector, which is shown in the pictures, is divided into dark and white bands. The borders of these bands are the isobars, set off through the equal intervals in P_{max} and P_{min} pressure range. Therefore it is evident that the width of the bands is directly connected with a pressure gradient. The presence of free vortices in the inner area of the collector greatly increases pressure gradient especially on its outlet (area between D and E in Fig.2). The bands in Fig.4b are narrower than in Fig.4a in this area. Resistance coefficient calculated for this area also leads to pressure gradient increase. In case of absence of the vortices, resistance coefficient equals f_g =306, but when there are 138 vortices, resistance coefficient equals f_g =2166. There is no opportunity to examine pressure distribution in a zone where the collector borders with HG element (the area inside quadrangle ABCD).

a) b)

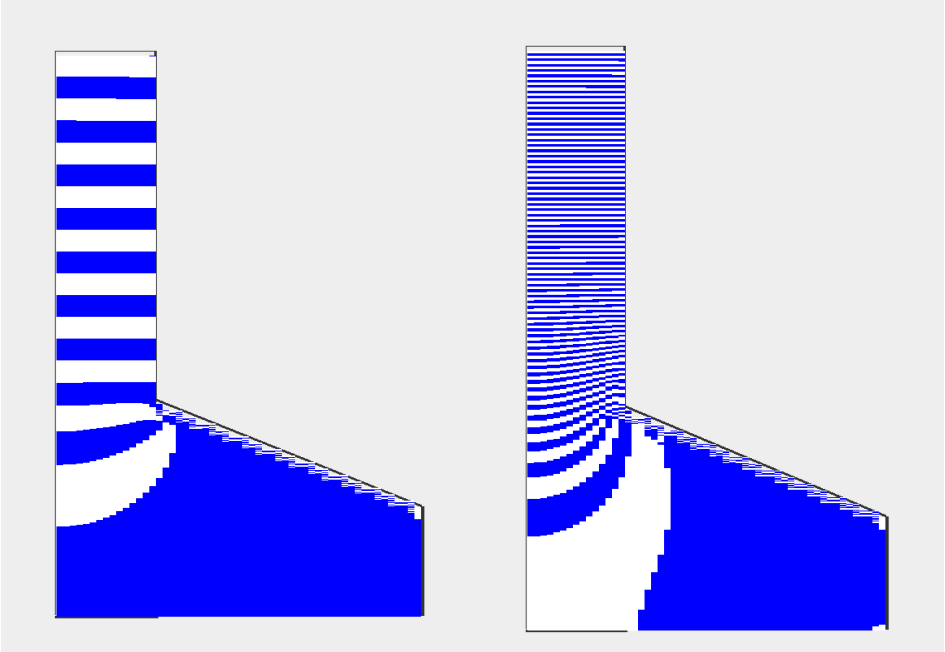

Fig.4. Bands, presenting equal intervals of pressure in the gathering collector:
a) There are no free vortices in the inner area of the collector,
b) There are 138 free vortices in the inner area of the collector.

All we can see is that the pressure gradient along the primary coolant flow direction a bit higher in Fig. 4b, as a band width is a bit narrower here. Changing the pressure can be examined in Fig. 5a and 5b.

Table 1 shows us how the free vortices availability in the gathering collector is connected with the resistance values in its various sections on the border with HG element. The first column indicates cross-section number, while the first line shows us free vortices quantity for resistance coefficient in this column. Section number 1 is a dead end zone in the gathering collector. In the collector we obtain the ultimate resistance coefficient on this zone outlet, i.e. in sections 19 and 20. Increasing free vortices number in the gathering collector doesn't lead to the steady increase of a resistance coefficient in all sections.

This fact proves that the simulated phenomena and collector pressure distribution are unsteady and resistance coefficients are statistically distributed. That's why the resistance coefficient in each section should be treated as its average value within our set of experiments. It also concerns the resistance coefficient on the gathering collector outlet. For the numerical experiments conducted for the free vortices cases 0, 138, 326, 1152 and 1758, resistance coefficient values equal 306, 2166, 5077, 2437, 16260 are obtained in accordance. The same situation can be observed when we estimate

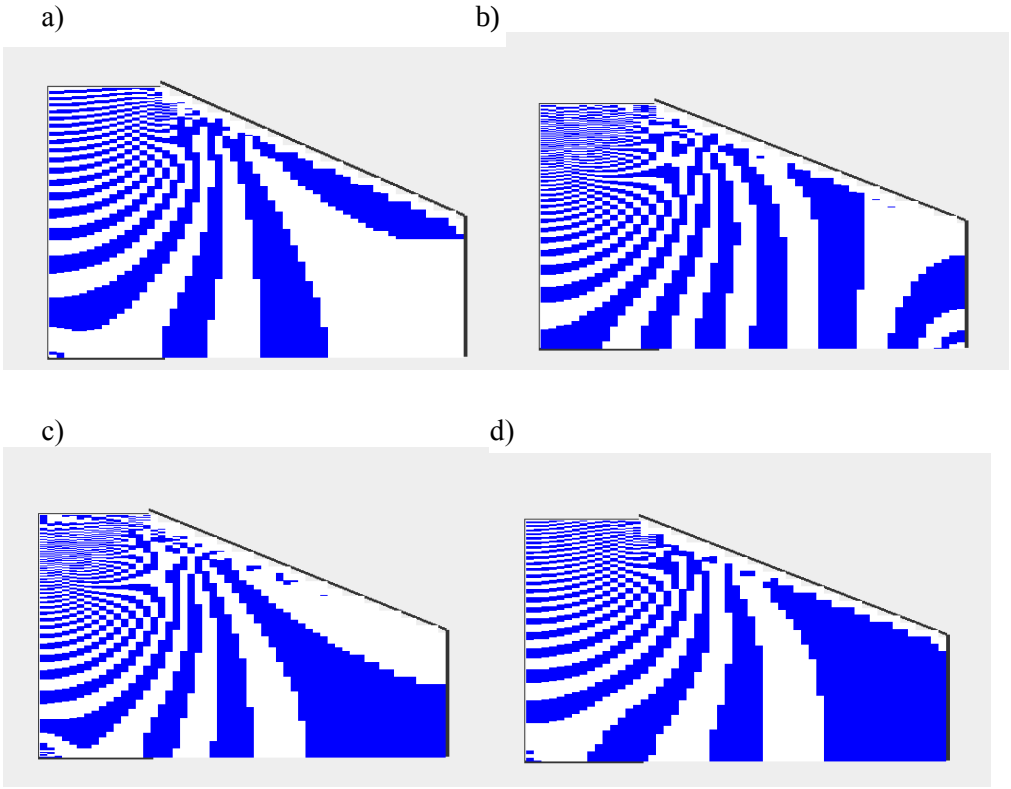

Fig.5. Bands of equal intervals of pressure in the gathering collector in the zone on the border with HG element. Free vortices in the collectors inner area:
a) no vortices , b) - 138 , c) 328 and d) – 1152 vortices.

the resistance coefficient in the distributing collector. On the collectors inlet, for the free vortices cases 0, 19, 47, 156 and 238, the resistance coefficient values equal 3968, 20862, 42840, 119998, 72013 are obtained accordingly. Their value is much higher upon the average here than on the gathering collector outlet. Table 2 shows us resistance coefficient values obtained in the distributing collector various sections on the HG element border zone. They are much higher than the gathering collector resistance coefficients almost everywhere and also change irregularly with an increase in the vortices number. In dead end zone (sections 17, 18, 19, 20) resistance coefficients are negative almost everywhere, which points to the fact that the pressure gradient slows down the flow and is directed towards the stream. However, in concordance with the classical hydrodynamics [4], the case, when a pressure changing gradient vector coincides with the flow vector direction, leads to the intensive vortex formation and as we can see in Fig. 6, the dead end zone vortices turn back to the middle and entry areas of the collector. Probably, this fact explains that the resistance coefficients in the distributing collector are much higher than in the gathering collector (see tables 1 and 2).

a) b)

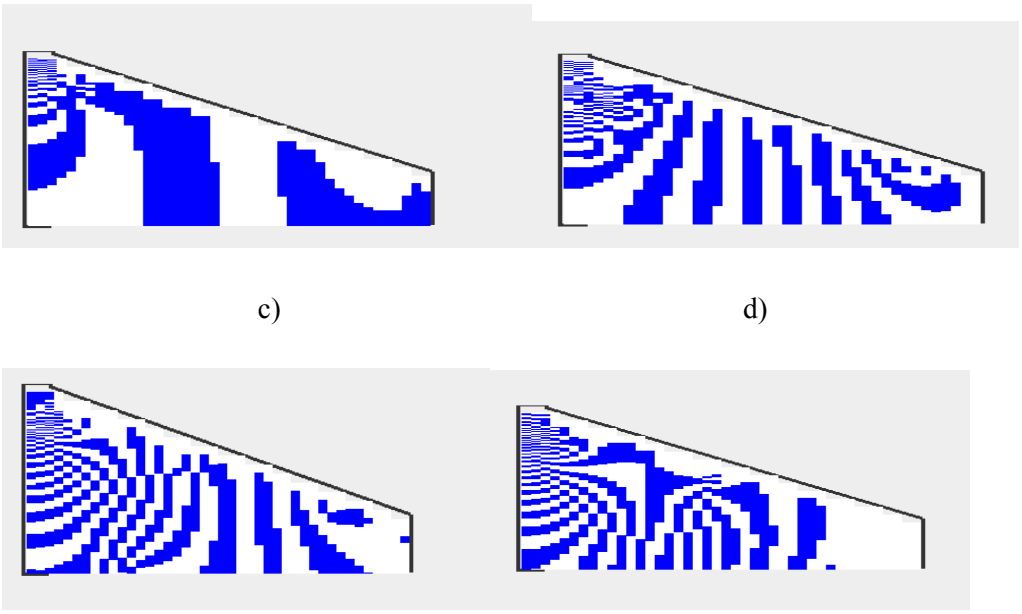

c) d)

Fig. 6 Bands of equal intervals of pressure in the distributing collector in the zone on the border with HG element. Free vortices in the collectors inner area: a) no vortices, b) -19, c) 47 and d) -156 vortices

Table 1.

№	0	138	326	1152	1758

1	6.9275e+04	6.3784e+05	3.9743e+04	4.7082e+04	1.4990e+04
2	6.9275e+04	2.1313e+05	2.3605e+02	1.8977e+04	9.2976e+03
3	3.2292e+03	8.0741e+04	1.5569e+03	1.6138e+04	2.0996e+04
4	2.1324e+03	4.1897e+04	1.8072e+03	1.0442e+04	2.3659e+04
5	1.1337e+03	2.6491e+04	2.7416e+03	8.3970e+03	1.7213e+04
6	2.2861e+03	1.8731e+04	3.1392e+03	6.9336e+03	1.2606e+04
7	2.7591e+03	1.4414e+04	3.4571e+03	6.0294e+03	9.7165e+03
8	3.1342e+03	1.1813e+04	3.4527e+03	5.4552e+03	8.1416e+03
9	3.1244e+03	9.9659e+03	3.6902e+03	5.1865e+03	7.0532e+03
10	3.3695e+03	8.7336e+03	3.9027e+03	5.1576e+03	6.4181e+03
11	3.5849e+03	7.8754e+03	4.1215e+03	5.2709e+03	6.0921e+03
12	3.8021e+03	7.2914e+03	4.3322e+03	5.3446e+03	5.9025e+03
13	4.0098e+03	6.9301e+03	4.5041e+03	5.4052e+03	5.8376e+03
14	4.1823e+03	6.6859e+03	4.7609e+03	5.5758e+03	5.8792e+03
15	4.4484e+03	6.6341e+03	5.1051e+03	5.8282e+03	6.0522e+03
16	4.8220e+03	6.7357e+03	5.5414e+03	6.1874e+03	6.3602e+03
17	5.3214e+03	6.8410e+03	5.9148e+03	6.4660e+03	6.5950e+03
18	5.7423e+03	7.4140e+03	6.6300e+03	6.8311e+03	6.9970e+03
19	6.6241e+03	5.1365e+05	1.0715e+06	4.0680e+05	2.5186e+06
20	8.7170e+04	5.1365e+05	1.0715e+06	4.0680e+05	2.5186e+06

Table 2.

№	0	19	47	156	238
1	4.6770e+04	2.3069e+05	7.1385e+05	3.0294e+06	1.7632e+06
2	2.6600e+04	1.1627e+05	6.4118e+05	2.9496e+06	1.6783e+06

3	1.3973e+03	5.7884e+04	6.6704e+05	2.9999e+06	1.6794e+06
4	1.0584e+04	5.5348e+04	6.2207e+05	2.9137e+06	1.6929e+06
5	1.2199e+04	5.3470e+04	5.2379e+05	2.8909e+06	1.7138e+06
6	1.3186e+04	5.5553e+04	4.2358e+05	2.9833e+06	1.7757e+06
7	1.4508e+04	5.7787e+04	3.7737e+05	2.8202e+06	1.8226e+06
8	1.5619e+04	5.9543e+04	3.1671e+05	2.1512e+06	1.7861e+06
9	1.7027e+04	6.2882e+04	2.8352e+05	1.6386e+06	1.8174e+06
10	1.8549e+04	6.6727e+04	2.5879e+05	9.2855e+05	1.8291e+06
11	2.0780e+04	7.4600e+04	2.9983e+05	1.1830e+06	2.0727e+06
12	2.3190e+04	8.2792e+04	3.3012e+05	1.2739e+06	2.3003e+06
13	2.6856e+04	9.5552e+04	3.7855e+05	1.3811e+06	2.5766e+06
14	2.7067e+04	9.4197e+04	3.6651e+05	1.3457e+06	1.9868e+06
15	1.9272e+04	6.6049e+04	2.5338e+05	9.8814e+05	1.1075e+06
16	1.4618e+04	5.0266e+04	1.9213e+05	4.6144e+05	8.3756e+05
17	-1.3051e+04	-3.5864e+04	-1.1963e+05	2.7811e+05	1.7349e+05
18	-3.4212e+04	-8.6685e+04	-2.6944e+05	1.7202e+05	-3.2275e+05
19	-2.3908e+04	-6.3891e+04	-2.0139e+05	6.5313e+04	-2.1841e+05
20	-2.3908e+04	-6.3892e+04	-2.0139e+05	6.5313e+04	-2.1841e+05

The distributing collector equal pressure interval bands on the HG element border zone, constructed for the free vortices various number, are shown in the Fig. 6. Here free vortices come off from the acute angle only, the same as angle D in the gathering collector (see Fig. 2). The first 150 vortices motion trajectory is shown in the Fig. 7.

Fig. 8 shows us the vorticity zone initial stage buildup in the gathering collector. Here vortices come off not only from the angle D, but also from the lattice bordering the collector and the HG element. In time, paths of these and other vortices fill almost all the gathering collector inner space. Probably, only upon that it is necessary to calculate the gathering collector resistance coefficients.

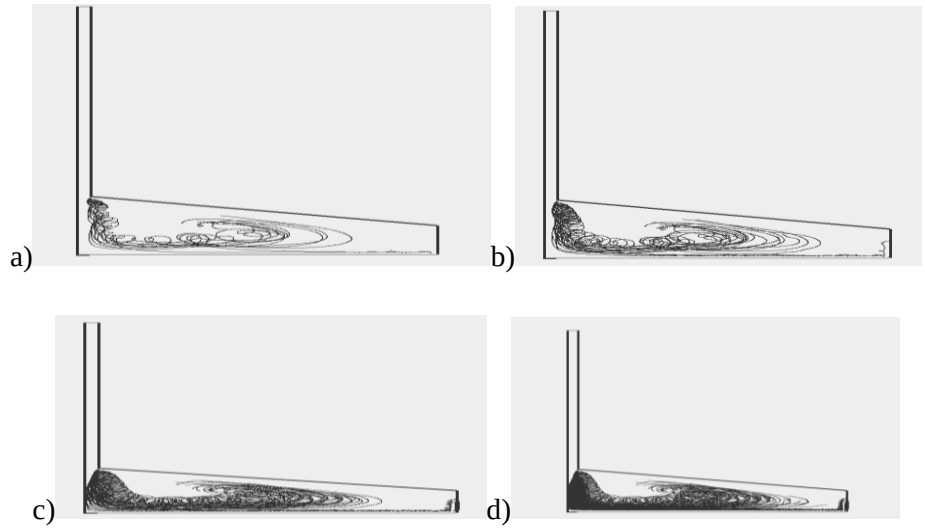

Fig.7 The first 10, 20, 50 and 150 vortices motion trajectories in the distributing collector

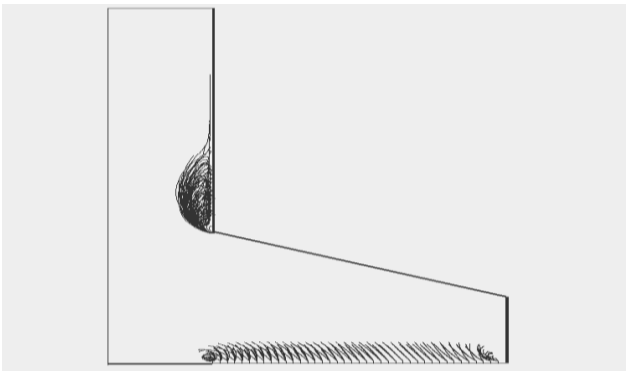

Fig.8 The gathering collector vorticity zone initial stage distribution when there are 138 free vortices

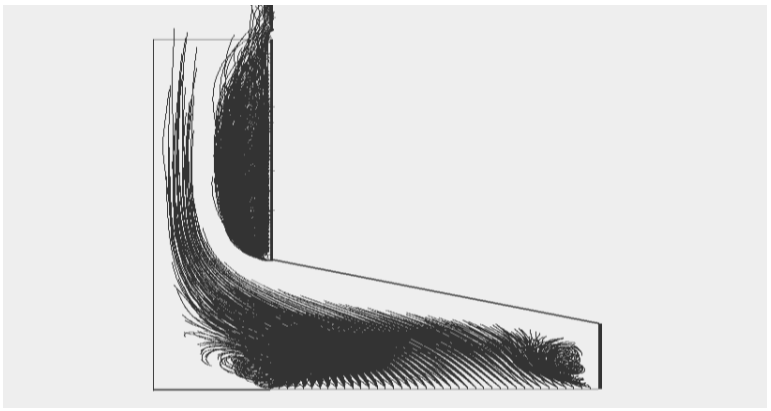

Fig.9 The gathering collector vorticity zone distribution when there are 1152 free vortices

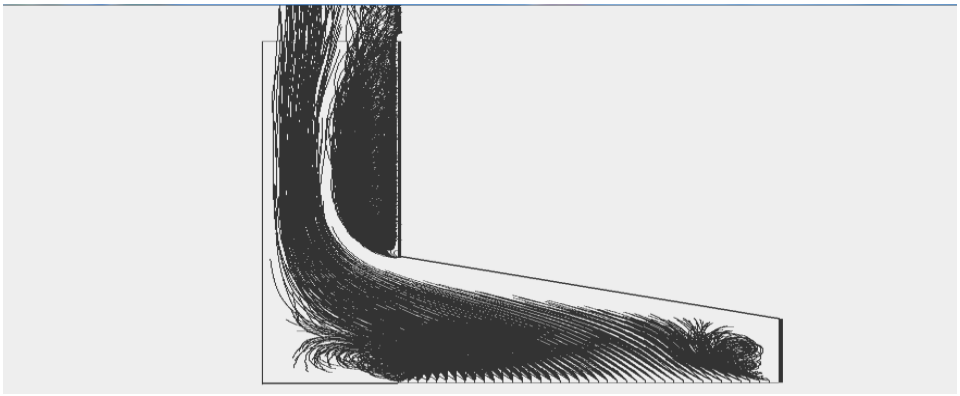

Fig.10 The gathering collector vorticity zone distribution when there are 1758 free vortices

Conclusion

Numerical experiments show us the considerable dependency of the pressure distribution and resistance coefficients on the gas flow vorticity degree in collectors. Resistance coefficients in a swirling flow are higher than in an irrotational flow in all cross-sections. Also conspicuous is the fact that resistance coefficient in distributing collector is much higher than in gathering collector almost in all sections. Probably, it is related to the fact that in the distributing collector dead end zone pressure gradient vector coincides with a gas flow velocity vector direction and is a powerful vorticity source in concordance with the dynamics of perfect liquid [4]. Moreover, the numerical experiments have failed to discover resistance coefficients simple linear dependency on the free vortices number in a gas flow in collectors. This fact proves that the examined phenomena are unsteady and probably it is required to use resistance coefficients arithmetical average value obtained from the set of experiments.

REFERENCES

1. Zhuchenko S. V. Numerical Simulation of Gas Dynamics and Heat Exchange Tasks in Fuel Assemblies of the Nuclear Reactors, Application of Mathematics in Technical and Natural Sciences AIP Conf. Proc. 1629, 135-145 (2014).
2. Belotserkovsky S.M., Nisht M.I. Excavate and steady air flow around the thin wings by ideal fluid. - Moscow: Nauka, 1978. - 352.
3. Schlichting G., Theory of the boundary layer. - Moscow: Nauka, 1974 - 712 p.
4. Herbert Oertel Prandtl - Fuhrer durch die Stromungslehre Grundlagen und Phanomene: Vieweg Verlag: Braunschweig 2002 ISBN 3-528-48209-5

Надійшла -13.11.2016.